MATERIALS PHYSICS AND MECHANICS RESEARCH ARTICLE

Submitted: July 12, 2025 **Revised: September 30, 2025** **Accepted: October 7, 2025**

About possibility of using the Roginsky-Schulz and Avrami-Erofeev equations in topokinetic analysis of carbothermic self-recovery of dispersed iron-graphite waste

L.A. Dan [1], V.A. Maslov [1], L.A. Trofimova [1], S.B. Kargin [1], V.G. Artiukh [2], D.A. Kitaeva [2] ✉, N.V. Korihin [2]

[1] Pryazovskyi State Technical University, Mariupol, Russia

[2] Peter the Great St. Petersburg Polytechnic University, St. Petersburg, Russia

✉ dkitaeva@mail.ru

ABSTRACT

Topokinetic analysis of experiment results on carbothermic self-healing of "wustite-graphite" dispersed samples particles was carried out. It was shown a dispersed iron-graphite waste contains metallic iron, iron oxide, carbon and impurities. Observations and calculations made in this work confirmed two-stage nature of process. The first initial stage of the process, at degrees of conversion less than 0.4, can be described by the Roginsky-Schulz or Avrami-Erofeev equations. Apparent activation energy of the initial stage of the process was calculated to be 141.34 kJ/mol. It was found that the Bell-Boudoir reaction is a limiting factor in the process.

KEYWORDS

topokinetic approach • graphite • dispersed iron-graphite waste • cast iron • carbothermic self-healing wustite-graphite

Funding. *This work has been supported by the grant of the Russian Science Foundation, RSF 25-19-00921.*

Citation: Dan LA, Maslov VA, Trofimova LA, Kargin SB, Artiukh VG, Kitaeva DA, Korihin NV. About possibility of using the Roginsky-Schulz and Avrami-Erofeev equations in topokinetic analysis of carbothermic self-recovery of dispersed iron-graphite waste. *Materials Physics and Mechanics*. 2025;53(4): 111–119. http://dx.doi.org/10.18149/MPM.5342025_9

Introduction

Dispersed iron-graphite waste (DIGW) is formed at all stages of cast iron processing. Their formation is associated with decrease in solubility of carbon with decreasing temperature and a number of other processes occurring in liquid iron [1,2]. They contain metallic iron, various iron oxides, carbon and impurities [2,3]. Electron microscopic studies [2] show that particles of dispersed liquid carbon dioxide are graphite plates, to a greater or lesser extent, covered with spherical oxide formations. The main part of oxide inclusions has a size of no more than 160 μm. They are tightly connected to surface of graphite particles and sometimes are located inside them.

This composition and structure of particles explain presence of unique combination of electrical and magnetic properties even in initial dispersed liquid gas phases [4–6]. When applied to graphite which consists of such particles and therefore has magnetic properties term 'magnetic graphite' is used [2]. In this case value of specific saturation magnetization (σ_s) depending on chemical composition of dispersed liquid carbon dioxide is in range from 22 to 45 A·m^2/kg and specific electrical resistance (ρ_v) is in range of

© L.A. Dan, V.A. Maslov, L.A. Trofimova, S.B. Kargin, V.G. Artiukh, D.A. Kitaeva, N.V. Korihin, 2025.
Publisher: Peter the Great St. Petersburg Polytechnic University
This is an open access article under the CC BY-NC 4.0 license (https://creativecommons.org/li-censes/by-nc/4.0/)

$(4.18–0.46)\cdot10^{-4}$ Ohm·m [2]. The authors position the materials as possessing properties such as radio shielding and radio absorption. An effective method for increasing specific saturation magnetization of DIGW is high-temperature heat treatment that results in formation of metallic iron. Due to this, value of σ_s increases to ~ 180 A·m^2/kg while maintaining low value of ρ_v ~ $2\cdot10^{-4}$ Ohm·m [2]. Efficiency of shielding and absorbing properties increases significantly. Based on this, it is relevant to study kinetic laws of metallization understanding of which will allow for effective control of the process [7].

Materials and Methods

DIGW is a mixture of iron oxides and reducing agent that is graphite. When this mixture is heated above certain temperature process of chemical reduction of iron oxides of dispersed DIGW to metallic iron by carbon contained in them begins. In essence, the process is a carbothermic self-healing one (CTSH). Recovery takes place with participation of solid and gas phases. Therefore, CTSH process can be considered as topochemical.

In [2,8,9] on study of carbothermic self-healing of dispersed DIGW, it was shown that the process occurs in two stages. At the first stage reduction of higher iron oxides to wustite occurs and at the second stage the reduction of wustite to metallic iron occurs. The first stage proceeds quickly. This is followed by induction period during which formation of metallic phase begins followed by its intensive growth. In [9], it is shown that newly formed iron can have a catalytic effect on the process but not immediately and after accumulation of certain minimum amount. Considering high dispersion of oxide component (average size of oxide particles did not exceed 160 μm) of processed material the maximum speed is achieved very quickly. After formation of continuous reaction front beginning of the process deceleration is recorded [9]. Since transformation of magnetite into wustite at temperatures of CTSH occurs almost completely already upon heating of particles to working temperature and the main time of CTSH particles of dispersed DIGW is occupied by reaction FeO → Fe [2,9,10]. This work focuses on topochemical analysis of this reaction occurring at CTSH.

To conduct CTSH of FeO particles wustite-graphite samples were prepared (63.8 % of FeO, 31.2 % of C, 5 % of impurities). Initial dispersed DIGW of mixing section with fraction of less than 160 μm was processed in a quartz reactor without air access for 1.5 h at 820 °C. At this temperature all iron oxides were converted into wustite [9]. Based on differential thermal analysis [9], temperatures above 960 °C were selected as working temperatures for conducting analysis of carbothermic self-healing: 970, 990, 1030 and 1050 °C.

In [2], microstructure of particles of wustite-graphite sample was analyzed after 5, 12, 20 and 40 min after start of carbothermic self-recovery at 1050 °C. Process FeO → Fe was characterized in early stages by formation of areas of metallic phase on surface of oxide. The process then developed with advancement of recovery front into particles and ended with complete recovery. In this case specific saturation magnetization increased monotonically from 0 (initial state) to 168.5 A·m^2/kg after its complete completion after 40 min [2].

Figure 1(a) shows set of curves of recovery degree of wustite (α) during course of experiment constructed according to data of [2]. During the first 5 min measurements were taken for every minute of the experiment then every 5 min. As can be seen from Fig. 1(a) increase in temperature causes shape of the curve to approach a sigmoid.

All curves have three more or less distinct sections, namely, incubation section in which iron nuclei are formed; acceleration section; section in which reaction rate gradually decreases. Similar appearance was shown by curves obtained in [11,12] during reduction of wustite with a hydrogen-helium mixture, in [13] during reduction of hematite to wustite with a gas mixture of N_2, CO, H_2 [13], and in [14] during reduction of hematite with a gas mixture of CO-CO_2.

Analysis of intensity of gas evolution and composition of gas phase for dispersed samples of "wustite-graphite" during CTSH carried out in [2] showed the following. Intensity of gas emission first increased and then decreased during the experiments. CO content was low for entire working temperature range at initial stage of the process. Then it increased and then CO/CO_2 ratio remained constant until end of the experiment. Based on processing of curves shown on Fig. 1(a) rate of recovery of wustite of dispersed samples of “wustite-graphite” at different temperatures of CTSH was calculated.

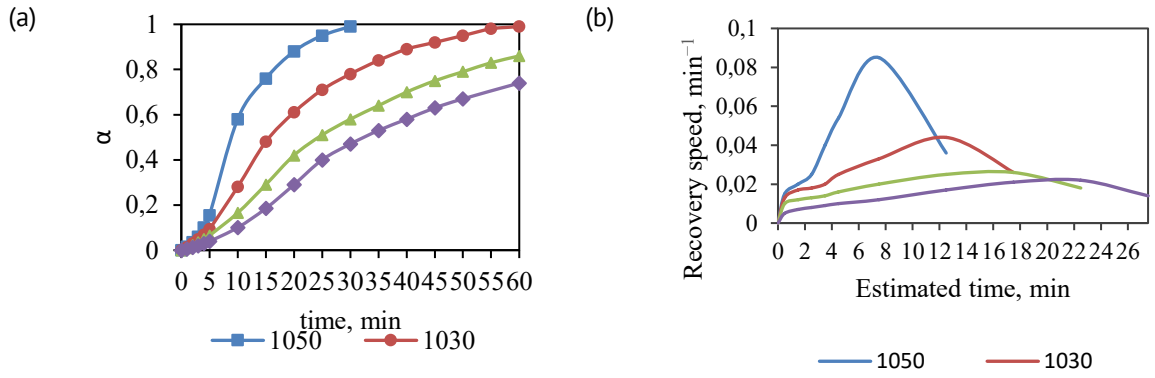

Fig. 1. Kinetics of CTSH of "wustite-graphite" sample [11] (a) and wustite recovery rate of dispersed "wustite-graphite" samples (b)

Calculated curves are shown on Fig. 1(b). Abscissa axis of graph shown on Fig. 1(b) shows calculated time values (average values of interval); ordinate axis shows average recovery rate in time interval. As with intensity of gas evolution, according to [2] rate of wustite recovery during CTSH increased at the beginning of the experiments and then decreased. Increase in temperature in the experiments in studied range leads to an increase in magnitude of recovery rate extremes and their earlier achievement. Thus, at temperature of 970 °C maximum rate of wustite reduction was 0.022 min^{-1} and it was achieved between the 20th and 25th min from beginning of the experiment; at 990 °C the maximum rate was 0.026 min^{-1} and it was achieved between the 15th and 20th min from beginning of the experiment; at 1030 °C the maximum rate was 0.044 min^{-1} and it was achieved between the 10th and 15th min from beginning of the experiment; at 1050 °C the maximum rate was 0.085 $min^{-1}$and it was achieved between the 5th and 10th min from beginning of the experiment. At the same time duration of incubation period decreased. These observations confirm statement about two-stage nature of carbothermic self-healing process made in [2] based on analysis of kinetic curves of CTSH of polydisperse DIGW as well as in studies [13–15].

Joint analysis of Fig. 1 allows to determine proportion of wustite that has transformed into metallic iron by time of reduction process transitions from the first to the second stage. For temperature of 1050 °C it is 0.4; for temperature of 1030 °C it is 0.4; for temperature of 990 °C it is 0.37; for temperature of 970 °C it is 0.36.

Results and Discussion

According to prevailing theory process of reduction of iron oxides by solid carbon is a process involving a gaseous reducing agent [16–18]. Reaction sphere contains solid and gaseous reagents, i.e. the process is topokinetic in nature [13,19]. This is also evidenced by sigmoid form of kinetic curves of CTSH of dispersed particles of "wustite-graphite" shown on Fig. 1(a) as well as CTSH curves of polydisperse DIGW in [2]. It should be kept in mind that the process can be limited both by gasification reaction of carbon contained in sample and by chemical reduction reaction. Taking these considerations into account in order to describe the process of CTSH a topochemical analysis of previously obtained results was carried out in this work.

Modern topokinetic approach to this type of process assumes their two-stage nature [14,15,19]. At the first stage, as a result of interaction of solid and gaseous phases nuclei of reaction product appear on surface of particles, they increase in size, and they merge. The second stage begins after continuous film of reaction product appears on solid particles. Then boundary of reaction proceeds moves deeper into the particles. Since processes occurring at different stages are different, attempts to combine entire process with one general equation led to need to introduce correction factors purpose of which is not to describe the process but to fit equation to obtained experimental curves.

Therefore, by analogy with [12,14,20] each experiment was conditionally divided into two stages, namely, at the first stage the rate increased due to increase of reaction surface and at the second stage the rate decreased due to its decrease. Due to low degree of conversion, the first stage can be called the initial stage, and the second stage can be called the main stage. These stages are separated by the maximum rate.

For topokinetic analysis of available experimental data the Roginsky-Schulz (Eq. (1)) [20] and Avrami-Erofeev (Eq.(2)) [21–23] equations were used in turn to compare results of the analysis:

$$\frac{d\alpha}{d\tau} = k \cdot \alpha^{2/3}; \quad (1)$$

$$\alpha = 1 - exp(-\beta\tau^n), \quad (2)$$

where α is degree of conversion, $d\alpha/d\tau$ is process speed (W), β is a constant that depends on both rate of nucleation and rate of growth of embryos, n is coefficient indicating geometric parameters of embryo growth.

According to [13], one-dimensional, two-dimensional, three-dimensional growth of embryos occurs at n = 1…2, n = 2…3 n = 3…4, respectively. In case when process can be described by Eq. (1) graph in coordinates $W(\alpha^{2/3})$ should have form of a straight line. After carrying out corresponding calculations graphs in coordinates of Roginsky-Schulz equation (Fig. 2) were obtained in form of four straight lines. This speaks in favor of assumptions made about the possibility of applying Roginsky-Schulz equation to the description of the process under consideration. Processing graphs on Fig. 2 allows calculating coefficients k in Eq. (1) for all experimental temperatures and their natural

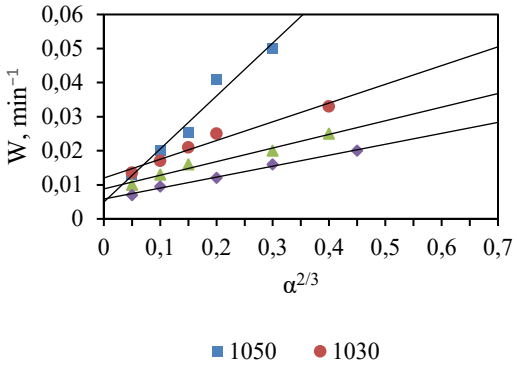

Fig. 2. Graphs in Roginsky-Schulz coordinates

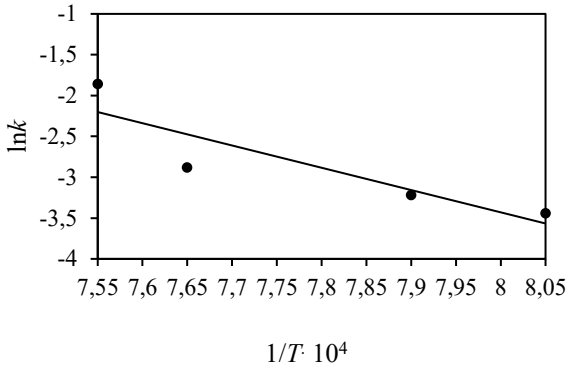

Fig. 3. Graph in Arrhenius coordinates constructed using data from Table 1

Table 1. Results of calculations of coefficients *k* in the Roginsky-Schulz equation

***T*, °C**	***k***	**ln*k***
1050	0.156	-1.858
1030	0.056	-2.882
990	0.04	-3.219
970	0.032	-3.442

logarithms (Table 1). Data from Table 1 is used to plot a graph in Arrhenius coordinates (Fig. 3) and calculate apparent activation energy of process E_a.

Based on obtained graph (Fig. 3) apparent activation energy of process of carbothermic self-healing of dispersed samples of "wustite-graphite" at the first stage was calculated: E_a = 216.16 kJ/mol. It should be noted that such a level of E_a indicates that the reducing agent, which in this case is graphite, has low activity. This is due to peculiarity of its formation at temperatures above 1500 °C. Only in presence of a certain amount of newly formed iron does the process gain noticeable speed. Author of work [24] also points to this.

Using graph shown on Fig. 3 value of k_0 in equation is determined:

$$k = k_0\, exp(-E_a/RT) \quad . \tag{3}$$

From Eq. (3) taking into account found value $k_0 = 2.6 \cdot 10^4$ expression is obtained:

$$k = 2.6 \cdot 10^4\, exp(-216.16/RT) \tag{4}$$

Rate of the process according to the Roginsky-Schulz equation:

$$W = 2.6 \cdot 10^4\, exp(-216.16/RT)\, \alpha^{2/3}. \tag{5}$$

From Eq. (5) degree of transformation:

$$\alpha = [0.867 \cdot 10^4\, exp(-216.16 \cdot 10^3/RT)\, \tau]^3. \tag{6}$$

To evaluate obtained result, experimental points (exp) and points calculated according to Eq. (6) (calc) are plotted on graph of $\alpha(\tau)$ dependence (Fig. 4). Analysis shown on Fig. 4 demonstrates that, contrary to assumptions made in [9], Roginsky-Schulz equation cannot be used for topokinetic analysis of the first stage of carbothermic self-healing of dispersed "wustite-graphite" samples.

Based on obtained results, the experimental data were processed using the Avrami-Erofeev equation. Evaluation of n and β indicators in Eq. (2) is usually carried out using the Hancock-Sharp method [13,14,25]. In accordance with this method, a graph of dependence of ln(-ln(1-α)) on lnτ was constructed and analyzed (Fig. 5(a)). From Fig. 5(a)

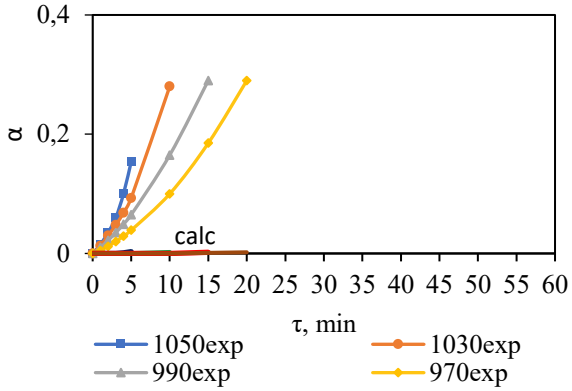

Fig. 4. Comparison of data obtained in the experiment and according to Roginsky-Schulz equation

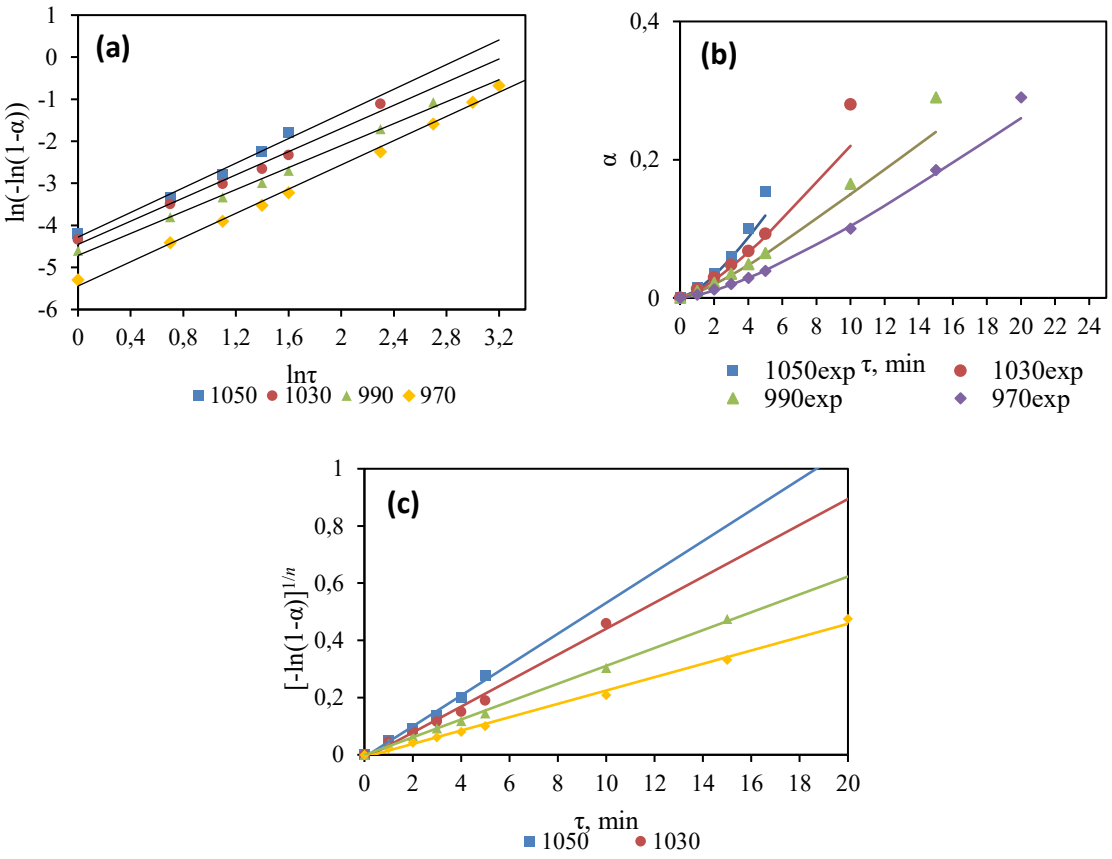

Fig. 5. (a) Dependence of function ln(-ln(1-*α*)) on ln*τ* for experimental conditions;
(b) comparison of data obtained during the experiment and in calculations using the Avrami-Erofeev equation;
(c) dependence of [-ln(1-*α*)]1/n on *τ* under experimental conditions

Table 2. Results of calculations of coefficients of the Avrami-Erofeev equation

No	*T*, °C	*n*	ln*β*	Correlation coefficient, *R*
1	1050	1.465	-4.425	0.990
2	1030	1.380	-4.589	0.994
3	990	1.305	-4.844	0.997
4	970	1.440	-5.585	0.998
Average value		1.398	-4.861	0.995

it follows that function ln(-ln(1-α)) on lnτ is linear at experimental temperatures, i.e., the Avrami-Erofeev equation can be used for the analysis. Based on the analysis of graphs shown on Fig. 5(a) n and β indicators were calculated, and the calculation results are presented in Table 2.

Comparison of results of applying Eq. (2) with experimental data was carried out by analyzing experimental (exp) and calculated curves (calc) shown on Fig. 5(b) and indicates that kinetic model very accurately (with average value of correlation coefficient R = 0.995) describes the process of nucleation and growth of the metallic phase on the surface of wustite particles. Obtained average value $n \approx 1.4$ indicates that process of FeO reduction occurs in kinetic region.

For further calculations the Avrami-Erofeev equation is transformed into form [13]:

$$[-ln(1-\alpha)]^{1/n} = k\tau. \quad (7)$$

Figure 5(c) shows graphical interpretation of Eq. (7) under experimental conditions. Coefficients k in Eq. (7) at different temperatures were calculated using slope of straight lines shown on Fig. 5. Calculation results are given in Table 3.

Table 3. Calculations result of coefficient k in of the Avrami-Erofeev equation (Eq. (7))

No.	T, °C	k	ln$k$
1	1050	0.0540	-2.919
2	1030	0.0454	-3.092
3	990	0.0312	-3.467
4	970	0.0233	-3.760

As in previous case to calculate apparent activation energy of process E_a graph in Arrhenius coordinates was constructed based on data in Table 3 (see Fig. 6). Calculation of E_a performed on the basis of Fig. 6 gives value of apparent activation energy of carbothermic self-recovery process of dispersed samples of "wustite-graphite" of 141.34 kJ/mol. Obtained values are in good agreement with data available in literature concerning reduction of wustite by graphite [24–26].

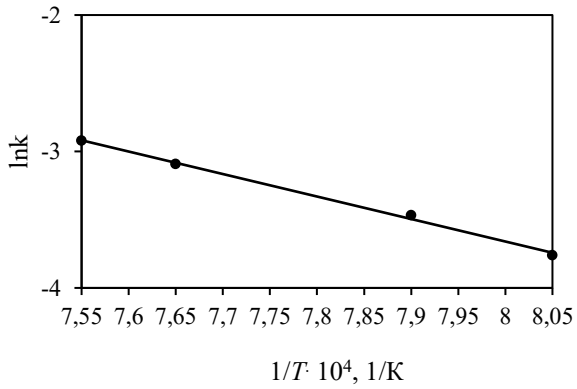

Fig. 6. Graph in Arrhenius coordinates constructed according to data shown in Table 3

In [27], it was found that apparent activation energy of graphite gasification process E_a is 444 kJ/mol. At the same time for complete understanding of the process kinetics [28–30], it is necessary to take into account fact that under considered conditions process

of oxide reduction occurs faster than reaction of CO formation [31–33]. Therefore, in this case it can be concluded that the process is limited by carbon gasification reaction [34,35].

Conclusions

Topokinetic analysis of the process of carbothermic self-healing of dispersed samples of "wustite-graphite" showed following:

1. The Avrami-Erofeev equation can be used in conjunction with the Sharpe-Hancock procedure to describe the process while the Roginsky-Schulz equation does not provide adequate description.
2. Calculated apparent activation energy of this process E_a is equal to 141.34 kJ/mol.
3. The process is limited by carbon gasification reaction.

CRediT authorship contribution statement

Leonid A. Dan: writing – review & editing; **Vladimir A. Maslov**: supervision; **Larisa A. Trofimova**: writing – original draft; **Sergey B. Kargin**: conceptualization; **Viktor G. Artiukh**: investigation; **Daria A. Kitaeva**: data curation; **Nikolay V. Korihin**: data curation.

Conflict of interest

The authors declare that they have no conflict of interest.

References

1. Petrov GV, Boduen AYa, Fokina SB, Popov AA. Chemical concentration of steel-making dusts. *Chernye Metally.* 2016;10: 65–68. (In Russian)
2. Dan L, Maslov V, Trofimova L, Cios G. The Formation, Properties and Use of Dispersed Iron-Graphite Metallurgical Waste. *Journal of Casting & Materials Engineering.* 2022;6(4): 81–92.
3. Chukaeva MA, Matveeva VA, Sverchkov IP. Complex processing of high-carbon ash and slag waste. *Notes of Mining Institute.* 2022;253: 97–104.
4. Li S, Zhang B, Wu D, Li Z, Chu S-Q, Ding X, Tang X, Chen J, Li Q. Magnetic Particles Unintentionally Emitted from Anthropogenic Sources. Iron and Steel Plants. *Environmental Science & Technology Letters.* 2021;8(4): 295–300.
5. Michalik JM, Wilczynska-Michalik W, Gondek L, Tokarz W, Zukrowski J, Gajewska M, Michalik M. Magnetic fraction of the atmospheric dust in Kraków – physicochemical characteristics and possible environmental impact. *Atmospheric Chemistry and Physics.* 2023;23(2): 1449–1464.
6. Aleksandrova TN, Chanturia AV, Kuznetsov VV. Mineralogical and technological features and patterns of selective destruction of ferruginous quartzites of Mikhailovskoye deposit. *Notes of Mining Institute.* 2022;256: 517–526.
7. Petrov G, Zotova I, Nikitina T, Fokina S. Sorption recovery of platinum metals from production solutions of sulfate-chloride leaching of chromite wastes. *Metals.* 2021;11(4): 569.
8. Cheremisina E, Cheremisina O, Ponomareva M, Bolotov V, Fedorov A. Kinetic features of the hydrogen sulfide sorption on the ferro-manganese material. *Metals.* 2021;11(1): 90.
9. Maslov VA, Trofimova LA, Makeev VE, Pustovalov YP. Differential thermal analysis of kinetics of carbothermic self-healing of dispersed wastes of metallurgical production. *Bulletin of Priazovskiy State Technical University. Series: Technical Sciences.* 2003;13: 76–79. (In Russian)
10. Sulimova MA, Sizyakov VM, Litvinova TE, Vasilyev VV. On possibility of the use of metallurgical production wastes as a sorbent in the industrial water cycle. *Chernye Metally.* 2016;8: 43–49. (In Russian)
11. Syrkov AG, Yachmenova LA. Features of obtaining metallurgical products under conditions of solid-state hydride synthesis. *Notes of Mining Institute.* 2022;256: 651–662.
12. El-Rahaiby SK, Rao YK. Kinetics of Reduction of Wustite by Hydrogen-Helium Gas Mixtures at Modest Temperatures. *Transactions of the Iron and Steel Institute of Japan.* 1980;20(5): 287–291.

13. Benoit J, Perry D, Mondal K. Fischer-Tropsch Synthesis in supercritical CO2 – Inhibition of CO2 selectivity for enhanced hydrocarbon production. *Fuel.* 2017;209: 383–393.
14. Yu J, Han Y, Li Y, Gao P, Li W. Mechanism and Kinetics of the Reduction of Hematite to Magnetite with CO-CO_2 in a Micro-Fluidized Bed. *Minerals.* 2017;7(11): 209–220.
15. Kapelyushin Y, Sasaki Y, Zhang J, Jeong S, Ostrovski O. Effects of Temperature and Gas Composition on Reduction and Swelling of Magnetite Concentrates. *Metallurgical and Materials Transactions B.* 2016;47: 2263–2278.
16 Seaton CE, Specht MI, Stellar D. Potential uses of flexicoke for iron ore pelletizing in the Venezuelan steel industry. *Transactions of the Iron and Steel Society of AIME*. 1991;12: 139–144.
17. Varon Cardona LM, Narita CY, Takano C, Breda Mourao M. Characterisation of coal-charcoal composite biocoke as a sustainable alternative for ironmaking. *Canadian Metallurgical Quarterly.* 2017;56(2): 190–198.
18. Mitchell AR, Parker RH. The reduction of SnO_2 and Fe_2O_3 by solid carbon. *Minerals Engineering.* 1988;1: 53–66.
19. Boldyrev VV. Mechanochemical processes with the reaction-induced mechanical activation. Chemo-mechanochemical effect. *Russian Chemical Bulletin.* 2018;67: 933–948.
20. Rozovsky AY. *Kinetics of topochemical reactions*. Moscow: Chemistry; 1974. (In-Russian)
21. Avrami M. Kinetics of Phase Change. I General Theory. *The Journal of Chemical Physics.* 1939;7(12): 1103–1112.
22. Wang H, Thomson WJ. Binary kinetics in the Y-Ba-Cu system: 2. Nanosized particles. *AIChE Journal.* 1995;41(7): 1790–1797.
23. Liu H, Sullivan RM, Hanson JC, Grey CP, Martin JD. Kinetics and Mechanism of the β- to α-$CuAlCl_4$ Phase Transition: A Time-Resolved 63Cu MAS NMR and Powder X-ray Diffraction Study. *Journal of the American Chemical Society.* 2001;123(31): 7564–7573.
24. Trushenski SP, Li K, Philbrook WO. Non-topochemical reduction of iron oxides. *Metallurgical Transactions.* 1974;5: 1149–1158.
25. Hancock JD, Sharp JH. Method of Comparing Solid-State Kinetic Data and Its Application to the Decomposition of Kaolinite, Brucite, and $BaCO_3$. *Journal of the American Ceramic Society.* 2006;55(2): 74–77.
26. Kargin S, Artyukh V, Ignatovich I, Dikareva V. Development and Efficiency Assessment of Process Lubrication for Hot Forging. *IOP Conference Series: Earth and Environmental Science.* 2017;90: 012190.
27. Rao YK. The kinetics of reduction of hematite by carbon. *Metallurgical Transactions.* 1971;2: 1439–1447.
28. Shen J-P, Mobley PD, Douglas LM, Peters JE, Lail M, Norman JS, Turk B. Mechanistic study of CO formation from CO_2 using a mixed-metal oxide of tin, iron, and aluminum. *RSC Advances.* 2014;4(85): 45198–45206.
29. Ha H, Yoo M, An H, Shin K, Han T, Sohn Y, Kim S, Lee S-R, Han JH, Kim HY. Design of Reduction Process of SnO2 by CH4 for Efficient Sn Recovery. *Scientific Reports.* 2017;7(1): 14427.
30. Chernousov PI. Recycling. *Technologies for processing and utilization of man-made formations and waste in ferrous metallurgy*. Moscow: Publishing House MISiS; 2011. (In Russian)
31. Chislavlev VV, Feiler SV. Study of iron and manganese recovery from metallurgical waste. In: Science and youth: problems, searches, solutions. In: Temlyantsev MV. (ed.) *Proceedings of All-Russian Scientific Conference of Students, Postgraduates and Young Scientists.* 2014. p.62–65. (In Russian)
32. Davydov SV. Phase equilibria in carbide region of iron-carbon phase diagram. *Steel.* 2020;1: 22–30.
33. Selivanov EN, Gulyaeva RI, Zaripov RZ, Sel'menskikh NI, Marshuk LA. Effect of calcium oxide on the structure and the thermal properties of granulated high-iron slags. *Russian Metall..* 2020;2020: 121–126.
34. Berdnikov VI, Gudim YA. Chemical reactions in carbon gasification processes. News of higher educational institutions. *Ferrous Metallurgy.* 2019;62(9): 705–712.
35. Kuznetsov YS, Kachurina OI. Thermodynamic analysis of iron oxide reduction processes using carbon and water vapor. News of higher educational institutions. *Ferrous Metallurgy.* 2019;62(5): 394–406.